TRENDS IN SCIENCES 2026; 23(12): 13743
https://doi.org/10.48048/tis.2026.13743
RESEARCH ARTICLE

The Polyherbal of Extract Ethanolic *Ocimum Sanctum, Clitorea Ternatea* and *Moringa Oleifera* Prevent Neuronal Apoptosis on the Alzheimer's Disease Model-Rat Pheochromocytoma Cell Line Mediated by Upregulation of ChAT and BDNF

Wilda Bunga Tina Sanjaya[1], Hevi Wihadmadyatami[1], Nishijima Kazutoshi[2,3], Dwi Aris Agung Nugrahaningsih[4], Rini Widayanti[5], Ulayatul Kustiati[6], Dinda Aliffia[1], Sadad Faisal Faiz[1] and Dwi Liliek Kusindarta[1,*]

[1]*Department of Anatomy, Faculty of Veterinary Medicine, Universitas Gadjah Mada, Yogyakarta 55281, Indonesia*
[2]*Center for Animal Resources and Collaborative Study, National Institutes of Natural Sciences, Okazaki 4448585, Japan*
[3]*National Institute for Physiological Sciences, National Institutes of Natural Sciences, Okazaki 4448585, Japan*
[4]*Department of Pharmacology and Therapy, Faculty of Medicine, Public Health, and Nursing, Universitas Gadjah Mada, Yogyakarta 55281, Indonesia*
[5]*Department of Biochemistry, Faculty of Veterinary Medicine, Universitas Gadjah Mada, Yogyakarta 55281, Indonesia*
[6]*Laboratory of Veterinary Pharmacology, Faculty of Veterinary Medicine, Universitas Brawijaya, Jawa Timur 65151, Indonesia*

([*]Corresponding author's e-mail: indarta@ugm.ac.id)

Received: 4 March 2026, Revised: 23 April 2026, Accepted: 3 May 2026, Published: 5 August 2026

Abstract

The progressive neurodegenerative condition known as Alzheimer's disease (AD) demonstrates intellectual processing deterioration, underscoring the need for new therapies. Polyherbal formulations offer synergistic, multi-target actions with low toxicity. While *Ocimum sanctum* shows neuroprotective potential, the combined effects with *Moringa oleifera* and *Clitoria ternatea* are unknown. This study evaluated their polyherbal formulation in trimethyltin (TMT)-induced PC-12 cells employed as an *in vitro* model of AD-related neurotoxicity. Phytochemical screening was performed by Thin Layer. Chromatography (TLC) and UV-Vis spectrophotometry. The optimal combination was determined from IC50 values via MTT assay. Cell proliferation was assessed by CCK-8, apoptosis by Hoechst staining, JC-1 fluorescence assay was applied to assess mitochondrial membrane potential (ΔΨm), and neurocognitive biomarkers Brain-Derived Neurotrophic Factor (BDNF) and Choline Acetyltransferase (ChAT) by ELISA. Ethanolic extract of polyherbal contained flavonoids 13.55% (w/w), phenols 7.53% (w/w), tannins 2.31% (w/w), saponins 0.75% (w/w), alkaloids 0.33% (w/w), steroids 0.24% (w/w), and terpenoids. The optimal ratio (*O. sanctum*: *M. oleifera*: *C. ternatea* = 7:2:1) at 65 µg/mL enhanced viability and proliferation, reduced nuclear fragmentation, and suppressed apoptosis. JC-1 staining showed preserved ΔΨm, indicating mitochondrial protection. BDNF and ChAT levels were significantly elevated, suggesting improved neurocognitive function. This polyherbal combination demonstrates synergistic neuroprotection and promising therapeutic prospect candidate for AD.

Keywords: Alzheimer's disease, Cell line, Holy basil, Phytochemical, Polyherbal

Introduction

The most common cause of dementia globally is Alzheimer's disease (AD), a serious neurological illness. Intracellular tau protein aggregation and extracellular amyloid-β (Aβ) plaque formation are two of AD's defining characteristics, leading to neuroinflammation and neuron death [1-4]. These structural changes in the brain are associated with clinical symptoms, which progress from mild cognitive impairment to severe dementia, leading to significant declines in daily functioning and individual independence [4-6].

The global prevalence of dementia-related AD was 50 million cases in 2020, with projections that this figure could triple by 2050 [7]. In Indonesia, demographic and healthcare challenges take significant contribute to the increasing prevalence of AD. Studies show that in Indonesia, as the elderly population increases, the number of AD sufferers tends to increase. This is also in line with the high rates of non-communicable diseases (NCDs), such as diabetes, stroke and hypertension, which are risk factors of cognitive decline and dementia [8,9]. National data indicate that in 2019, 1 million people in Indonesia were living with dementia caused by AD [8].

Recently, AD therapies such as donepezil, rivastigmine, and galantamine work by increasing acetylcholine levels, one of neurotransmitters that plays a significant role in cognitive processes, including learning and memory, whereas the expression of acetylcholine is generally decreased in individuals with AD [10]. Administration of these medications could reduce clinical symptoms and improves cognitive abilities, with responses varying widely between individuals; however, it does not delay the disease severity and progression. Furthermore, the side effects, such as gastrointestinal problems and neuropsychiatric symptoms, also appear with prolonged medication administration [11]. This situation was urgently needed for new therapeutic strategies with non-pharmacological interventions such as cognitive stimulation therapy, lifestyle modification, and herbal remedies that can enhance the effectiveness of pharmacological treatments [12].

Medicinal herbs have emerged as promising candidates for new approaches to medication and/or palliative regimens, due to their rich phytochemical composition and synergistic bioactivities. *Ocimum sanctum* (*O. sanctum*) has been reported for its potent antioxidant, anti-inflammatory, anti-apoptotic, which may counteract oxidative stress, neuroinflammation, prevent neuronal dead and neuronal regeneration in AD [13-15]. *Clitoria ternatea* (*C. ternatea*) contains flavonoids and anthocyanins [16-18], which may help with memory-enhancing and neuroprotective effects. Meanwhile, *Moringa oleifera* (*M. oleifera*) is abundant in polyphenols, vitamins, and isothiocyanates, providing strong free radical scavenging activity [19]. While each of these medicinal plants has demonstrated neuroprotective potential individually, the present study adopts a polyherbal approach based on the principle of polyherbalism, whereby the combination of multiple herbs may yield synergistic or additive effects that enhance overall therapeutic efficacy. The combination of these ethanolic extracts is further justified by their complementary pharmacological activities, enabling the simultaneous modulation of multiple pathological mechanisms associated with Alzheimer's disease, particularly in the context of *in vitro* AD-related neurotoxicity, including oxidative stress, neuroinflammation, cholinergic dysfunction, and neuronal apoptosis. Moreover, such combinations may enhance the bioavailability and overall biological activity of phytoconstituents through synergistic interactions. Despite extensive evidence supporting the individual effects of these herbs, studies investigating their combined effects remain limited, thereby highlighting a significant research gap [20]. This research was aimed to explore the mechanism of polyherbal (combination of *O. sanctum, C. ternatea*, and *M. oleifera* - EEOCM) use as an emerging therapeutic candidate for Alzheimer's disease.

Materials and methods

Ethical approval

This research was executed under oversight of institutional ethical guidelines and received approval from the Board of Ethical Review of the Faculty of Veterinary Medicine, Universitas Gadjah Mada (Permission No. 88/EC-FKH/Int./2025).

Plant material and extraction

The dried simplicia of *O. sanctum, M. oleifera leaves, and C. ternatea* blume were purchased from CV

Merapi Herbal, located in Yogyakarta, Indonesia. Ninety six percent ethanol solution (Merck, Darmstadt, Germany) employed for extraction process of the formulation, a maceration approach was used for the extraction. Four liters of ethanol were used to soak 300 g of each dried item, out of a total of one kilogram. After the maceration process, evaporation was carried out using a Heidolph rotary vacuum evaporator (Schwabach, Germany) to concentrate the filtrate under lower pressure, producing a thick, paste-like semisolid extract.

Calculation of polyherbal EEOCM formulation

The formulation of the polyherbal extract was determined using the inhibitory concentration (IC_{50}) fraction method, in which the potency of each plant extract was expressed as the reciprocal of its IC_{50} value ($1/IC_{50}$). This approach ensures that extracts with stronger activity (lower IC_{50}) contribute a greater proportion to the final formulation. The fraction of each component was calculated using the formula:

$$fn = \frac{1/IC50n}{\sum(1/IC50j)} \text{ [21]} \quad (1)$$

Fn : The fraction of the n-th extract
IC50n : The IC_{50} value of the n-th extract
∑(1/IC50j) : The sum of the reciprocals of all IC_{50} values

The interaction between the individual plant extracts within the polyherbal formulation was assessed using Combination Index (CI) approach, as the model was developed by Chou and Talalay. The CI framework calculated according to the following Eq.(2):

$$CI = \sum_{i=1}^{n} \frac{di}{Di} \text{ [22]} \quad (2)$$

di : The concentration of the i-th extract in the combination that produces a given effect
Di : The concentration of the same extract alone

Ethanolic extract identification on the EEOCM

Spectrophotometry UV-Vis

Flavonoid

A weighed portion of 50 mg ethanolic extract of the polyherbal was introduced into a sterile tube to serve as test sample. To initiate the colorimetric reaction, 0.3% sodium nitrite ($NaNO_2$; Merck, Darmstadt, Germany) prepared in a 5% solution was included. After 5 min of being incubated, 0.6 milliliters of 10% aluminum chloride ($AlCl_3$; Merck, Darmstadt, Germany) was introduced, followed by an additional 5-minute reaction period. Subsequently, an aliquot of 2 mL of one molar NaOH (Merck, Darmstadt, Germany) was incorporated, after that process result solution was brought into a overall concoction of 10 milliliters with deionized aqueous medium. The blended solution was homogenized, pipetted into a quartz cell, and the measurement of absorbance was carried out at a wavelength of 510 nm employing a UV-Visible spectrophotometer.

Phenol

A weighed portion of 50 mg ethanolic extract of the polyherbal was introduced within a reaction tube. An additional 7.5 mL of filtered water along with Folin–Ciocalteu reagent an equal volume of 500 µL (Sigma, Burlington, MA, USA) were introduced. The concoction was equilibrated and maintained for 10 min under ambient conditions. to facilitate the initial reaction. Subsequently, an aliquot of a 20% (w/v) sodium carbonate solution an equal volume of 1.5 milliliters of (Merck, Darmstadt, Germany) incorporated then, final concoction will be brought into 10 mL with distilled water. The mixture was thoroughly homogenized, and spectral measurement was determined at a wavelength of 760 nm employing a UV-Visible spectrophotometer.

Tannin

A weighed portion of 50 mg ethanolic extract of the polyherbal maintained. Diethyl ether in the volume of 10 milliliters (Merck, Darmstadt, Germany) introduced within the sample, which was then being equilibrate in about 20 h. Once traces of diethyl ether were eliminated, the remaining residue was reconstituted with 10 mL of distilled water. Folin–Ciocalteu reagent an equal volume of 10 mL (Sigma,

Burlington, MA, USA) introduced to the solution, followed by vigorous mixing and a 5-minute incubation period. Subsequently, sodium carbonate solution in the volume of 2 mL of a 20% (w/v) (Merck, Darmstadt, Germany) incorporated. A 30-minute incubation period was applied to the reaction mixture prior to spectral measurement at 760 nm employing a UV-Visible spectrophotometer.

Alkaloid

A weighed portion of 50 mg ethanolic extract of the polyherbal was subjected to mixing with a 2-normal HCl solution (Sigma, Burlington, MA, USA). The obtained solution washed three times by a volume of 10 mL aliquots of chloroform. The acidic medium was then neutralized by the introduction of sodium hydroxide zero-point one molar solution (NaOH; Sigma, Burlington, MA, USA). Once the pH reached neutrality, 5 mL of phosphate-buffered saline and Bacillus Calmette–Guérin (BCG) reagent in the volume of 5 mL (Sigma, Burlington, MA, USA) were introduced, followed by 5 mL of chloroform. Magnetic stirring was operated at 500 rpm for of 15 min. The chloroform phase was then isolated and evaporated to dryness under a nitrogen stream, and the residue was re-dissolved in chloroform to a overall volume of 5 mL. spectral measurement was performed within 470 nm on a UV-Visible spectrophotometer.

Saponin

A weighed portion of 50 mg ethanolic extract of the polyherbal was prepared as a combination with 2 milliliters of 25% H_2SO_4 (Sigma, Burlington, MA, USA) and processed under steam sterilization conducted at 110 °C for a 120-minute interval. The mixture was then extracted with ether, and the resulting filtrate was dried. After the the mixture received 1 mL of deionozed water, vortex extraction was performed for 5 min. The mixture was subsequently homogenized, followed by supplementation with 50 milliliters 4-methoxybenzaldehyde (Sigma, Burlington, MA, USA), followed by a 10-minute resting period. Afterward, 2 milliliters of H_2SO_4 at 50% concentration (Sigma, Burlington, MA, USA) poured in, followed by maintaining the blend at 60° in a temperature-controlled condition for ten min, subsequently, concoction overall volume brought into 10 milliliters with distilled water in a standard flask, followed by a five-fold dilution. The spectral was then measured at 435 nm using a UV-Visible spectrophotometer.

Thin layer chromatography

The steroid and terpene content of the polyherbal ethanolic extract was analyzed using thin-layer chromatography (TLC). A 1 mg portion of the polyherbal extract was dispersed with one milliliter of ethanol, then underwent ultrasonic waves for 60 min. The sample was subsequently spun in a centrifuge, agitated with a vortex, and left to steep for 24 h. From this mixture, 100 µL was taken and deposited onto a fluorescent silica gel TLC plate stationary phase of thin-layer chromatography plate, in combination with a 60% pure β-sitosterol reference solution (Sigma, Burlington, MA, USA). Chromatographic development was carried out in a saturated chamber containing a toluene/ethyl acetate solvent system at a 93:7 (v/v) proportion. After chromatographic separation, visualization was performed by spraying the plate with Liebermann–Burchard reagent and heating at 110 °C for a duration of 2 min (Sigma, Burlington, MA, USA). Eventually, the spectral measurement of the spots was analyzed at 340 nm using a UV-visible spectrophotometer.

Maintenance of Rat Pheochromocytoma cell line (PC-12)

The American Type Culture Collection (ATCC, Manassas, VA, USA) made available of the Rat Pheochromocytoma cell line. Those were kept in T-75 flasks designed for cell cultivation, filled with Dulbecco's Modified Eagle Medium (DMEM; Gibco, Auckland, New Zealand) augmented alongside 250 microlitres of amphotericin B (Gibco, Langenselbold, Germany), 5 mL of fetal bovine serum (Capricorn, Ebsdorfergrund, Germany), 2.5 mL of horse serum (Capricorn, Ebsdorfergrund, Germany), and 5 hundred microlitres of penicillin–streptomycin (Capricorn, Ebsdorfergrund, Germany) in a total of complete medium of 50 mL. The cultures were maintained under controlled conditions incubated at 37° under a moist air chamber mixture with 5% CO_2. When the cells had attained around 80% confluence, subculturing was done.

Development and group design of *in vitro* model of AD-related neurotoxicity on the Rat Pheochromocytoma cell line (PC-12)

Making *in vitro* cells model of AD was established by exposing PC-12 cells (at a minimum of 80% confluence) to trimethyltin (TMT;Sigma-Aldrich, Langenselbold, Germany) 24 h at an equilibrium concentrate of 10 μM. The TMT crystals were blended in Dulbecco's phosphate-buffered saline (DPBS) (Sigma-Aldrich, Langenselbold, Germany) then, sterilized through a Millex syringe filter (Sigma-Aldrich, Langenselbold, Germany), after which the solution was mixed with complete culture medium prior to treatment. Cells were divided into several experimental groups, including a normal control group (untreated), a TMT-treated group without intervention defined as the disease control, a donepezil-treated group serving as the positive control, and treatment groups receiving the polyherbal formulation at various concentrations. Donepezil was included to validate the experimental model and to provide a reference for neuroprotective effects under *in vitro* AD-related neurotoxicity conditions.

Cell viability assay

A population density of 30,000 PC-12 cells in each culture chamber was applied to dispense in 96-well plates. The cells were exposed to either 1 μM donepezil hydrochloride (Sigma, Langenselbold, Germany), 10 μM trimethyltin (TMT; Sigma-Aldrich, Langenselbold, Germany), or polyherbal extract at doses of 32.5, 65, and 130 μg/mL after a 24-hour period. Following treatment, the growth medium solution was aspirated, then each culture chamber was rinsed with Dulbecco's phosphate-buffered saline (DPBS). Prior to the addition of the MTT reagent, images of each experimental group were captured using an inverted microscope with the aim of assesing the morphological characteristics of the cells. Each well was then incubated with ten percent of MTT solution (3-(4,5-dimethylthiazol-2-yl)-2,5-diphenyl tetrazolium bromide; Roche, Mannheim, Germany) prepared in growth medium and the cells were incubated under standard conditions (37 °C) for 4 h. Once incubation was complete, the culture growth medium containing MTT was removed, a volume of 100 μL dimethyl sulfoxide was applied to each well to ensure complete dissolution of the formed formazan deposits. The optical density was recorded at 595 nm using a microplate reader. The percentage of viable cells was calculated using the Eq. (3) below:

$$Cell\ Viability\ (\%) = \frac{(Treated\ Cell\ Absorbance - Control\ Media\ Absorbance)}{(Control\ Cells\ Absorbance - Control\ Media\ Absorbance)} \times 100\%\ [13] \quad (3)$$

Cells proliferation assay

A population density of 30,000 PC-12 cells in each culture chamber was applied to dispense in 96-well plates. Cells were exposed to or left untreated with 10 μM trimethyltin (TMT), 1 μM donepezil hydrochloride, or polyherbal extract at concentrations of 32.5, 65, and 130 μg/mL. Following treatment, 10% Cell Counting Kit-8 (CCK-8) reagent (Abbkine, Wuhan, China) prepared in complete medium was introducedto each well. Post-incubation at 37 °C for around 2 h, the sample's spectrophotometric reading was determined at 450 nm with a multiwell plate reader. Proliferative activity was calculated using the Eq. (4) below:

$$Proliferation\ rate\ (\%) = \frac{(Treated\ Cell\ Absorbance - Control\ Media\ Absorbance)}{(Control\ Cells\ Absorbance - Control\ Media\ Absorbance)} \times 100\%\ [13] \quad (4)$$

Assessment of nuclear changes and cell population by Hoechst 33342 staining

PC-12 cells 50,000/well were distributed onto coverslips placed in 24-well plates and incubated for 24 h. Upon reaching approximately 50% confluence, the cells were subjected for 24 h with or without 10 μM trimethyltin (TMT), 1 μM donepezil hydrochloride, or polyherbal extract at concentrations of 32.5, 65, and 130 μg/mL. After treatment and being cleaned with DPBS, the cells were fixed for 15 min using ice-cold 70% ethanol. Following the discharge of the fixative, the cells proceed to three DPBS washes before being incubated with 200 μL of Hoechst 33342 staining solution (1 μg/mL) for 10 min in the dark. Following a final 5-minute DPBS wash, nuclear morphology was observed using a confocal microscope (Leica, Wetzlar, Germany). The image data were acquired further assessed using ImageJ software, where cells were scored

based on total cell count, nuclear fragmentation, and the presence of pyknotic nuclei.

After Hoechst 33342 staining, fluorescent images were acquired from 5 randomly selected fields per treatment group. Nuclear morphology was assessed using a semi-quantitative scoring system, in which scoring was based on the cumulative cell number, presence of nuclear fragmentation, and pyknosis. The criteria were defined as follows [23].

- +++++: >200 cells, without signs of nuclear fragmentation or pyknosis.
- ++++: >150 cells, Without signs of nuclear fragmentation or pyknosis.
- +++: >130 cells, with minimal nuclear fragmentation.
- ++: >130 cells, with extensive nuclear fragmentation.
- +: ≤100 cells, with extensive nuclear fragmentation.

In parallel, ImageJ software (NIH, Bethesda, MD, USA) was used to directly quantify the total number of nuclei per field, providing an objective measure of cell density across groups. This combined approach enabled both semi-quantitative evaluation of nuclear morphology and quantitative analysis of total cell counts.

JC-1 Staining

In 24-well plates, a population density of PC-12 cells (5×10^4 cells/well) were planted on coverslips and incubated for 24 h. Upon reaching approximately 50% confluence, the cells were exposed for 24 h to either 10 μM trimethyltin (TMT), 1 μM donepezil hydrochloride, or polyherbal extract at concentrations of 32.5, 65, and 130 μg/mL. Following treatment, excess dye was removed by washing the cells with JC-1 assay buffer, after which a 2% JC-1 probe staining solution (Elabscience, Wuhan, Hubei, China) was introduced to each well. Following the incubation of the cells in a dark environment during a 20-minute incubation at 37 °C. Residual JC-1 solution was eliminated by buffer treatment after the staining solution was withdrawn. The potential of the mitochondrial membrane was evaluated by fluorescence imaging using a confocal microscope (Leica, Wetzlar, Germany). ImageJ (NIH, USA) program was employed to quantify fluorescence levels, and the red-to-green fluorescence ratio was calculated to determine mitochondrial functional integrity.

Cell lysates preparation

PC-12 cells were cultured at 5×10^5 cells per well in 6-well plates for 24 h, followed by washing with DPBS. The cells were then treated for an additional 24 h with or without 10 μM trimethyltin (TMT), in the presence of either 1 μM donepezil hydrochloride or polyherbal extract at concentrations of 32.5, 65, and 130 μg/mL. Following treatment, the cells were detached using a sterile cell scraper, rinsed, and lysed by sonication. The resultant lysates were spun down at 10,000 rpm for ten min at 4 °C, and the supernatants were collected for subsequent analyses.

Enzyme Linked Immunosorbent Assay (ELISA) for BDNF and ChAT

Commercial ELISA kits (Elabscience, Wuhan, Hubei, China) were used to measure the amounts of brain-derived neurotrophic factor (BDNF) and choline acetyltransferase (ChAT) expressed in the cell lysates in following the kit provider's guidelines. A Tecan Spark 20M reader (Männedorf, Switzerland) was employed to assess the 450 nm absorbance.

Results and discussion

Polyherbal formulation of EEOCM

The IC_{50} values of *Ocimum sanctum* (187 μg/mL), *Moringa oleifera* (984.9 μg/mL), and *Clitoria ternatea* (1,746 μg/mL) were obtained from a previous study. Based on IC_{50} fractionation, the theoretically optimal combination ratio was calculated to be 77.1%:14.6%:8.3%. For experimental formulation, a ratio of 70%:20%:10% was applied. The interaction of the combined extracts, assessed using the Chou–Talalay combination index (CI) method, yielded a CI value of 0.004. According to the CI interpretation scale (CI < 1 = synergism, CI = 1 = additive effect, CI > 1 = antagonism), this result demonstrates a highly synergistic effect [22].

Phytochemical identification of the polyherabal EEOCM

The phytochemical analysis of the polyherbal ethanolic extract revealed a diverse composition of

secondary metabolites. The UV-Vis spectrophotometry verified the existence of flavonoids, tannins, phenols, alkaloids, and saponins, while TLC analysis identified steroids and terpenoids (**Tabel 1**). Together, these results indicate that the extract contains multiple classes of bioactive compounds with potential pharmacological relevance. The phytochemical quantification of the polyherbal extract revealed that flavonoids were the most abundant constituent 13.55% (w/w), followed by phenols 7.53% (w/w) and tannins 2.31% (w/w). Lower concentrations were observed for saponins 0.75% (w/w), alkaloids 0.33% (w/w), and steroids 0.24% (w/w). In addition, terpenoids were detected qualitatively as positive by TLC analysis.

The presence of bioactive compounds such as flavonoids, phenolics, and alkaloids in the polyherbal extract suggests potential central nervous system activity, as several compounds within these classes have been reported to cross the blood-brain barrier, although their permeability may vary depending on molecular structure and metabolic transformation [24-26]. However, further studies are required to directly evaluate their blood-brain barrier permeability and bioavailability.

Table 1 Identification of Bioactive Compounds in Polyherbal Extract Using UV-Vis Analysis and TLC.

Compound name	Concentration	Unit	Metode
Flavonoid	13.55	%(w/w)	UV-Vis
Phenol	7.53	%(w/w)	UV-Vis
Tanin	2.31	%(w/w)	UV-Vis
Saponin	0.75	%(w/w)	UV-Vis
Alkaloid	0.33	%(w/w)	UV-Vis
Steroid	0.24	%(w/w)	TLC
Terpenoid	Positive	-	TLC

Polyherbal EEOCM preserved viability, and supported proliferation TMT-induced alzheimer diseases on the PC12 cells

The present study demonstrates that the combination of polyherbal ethanolic extracts of *Ocimum sanctum, Clitoria ternatea,* and *Moringa oleifera* provide mechanisms of the neuroprotective effects on the increasing of viability, proliferation and inhibition of apoptotic on the Alzheimer's Disease Model-Rat Pheochromocytoma cell line (PC-12 cell line). In the presence of EEOCM the *in vitro* model of AD-related neurotoxicity provides more strengthen of viability and proliferation, this results in line with the morphological analysis. The effect of the polyherbal EEOCM extract on PC12 cell viability was assessed using the MTT assay under TMT-induced neurotoxic conditions. Exposure to TMT alone markedly decreased cell viability compared with untreated controls, confirming its cytotoxic impact. In contrast, treatment with the polyherbal extract mitigated this reduction in a concentration-dependent manner, with the 65 µg/mL dose exhibiting the greatest protective effect. Donepezil treatment, included as a reference, also improved cell viability, thereby supporting the validity of the assay (**Figure 1(a)**). Collectively, these findings indicate that the polyherbal formulation exerts a significant cytoprotective influence against TMT-induced damage in PC12 cells.

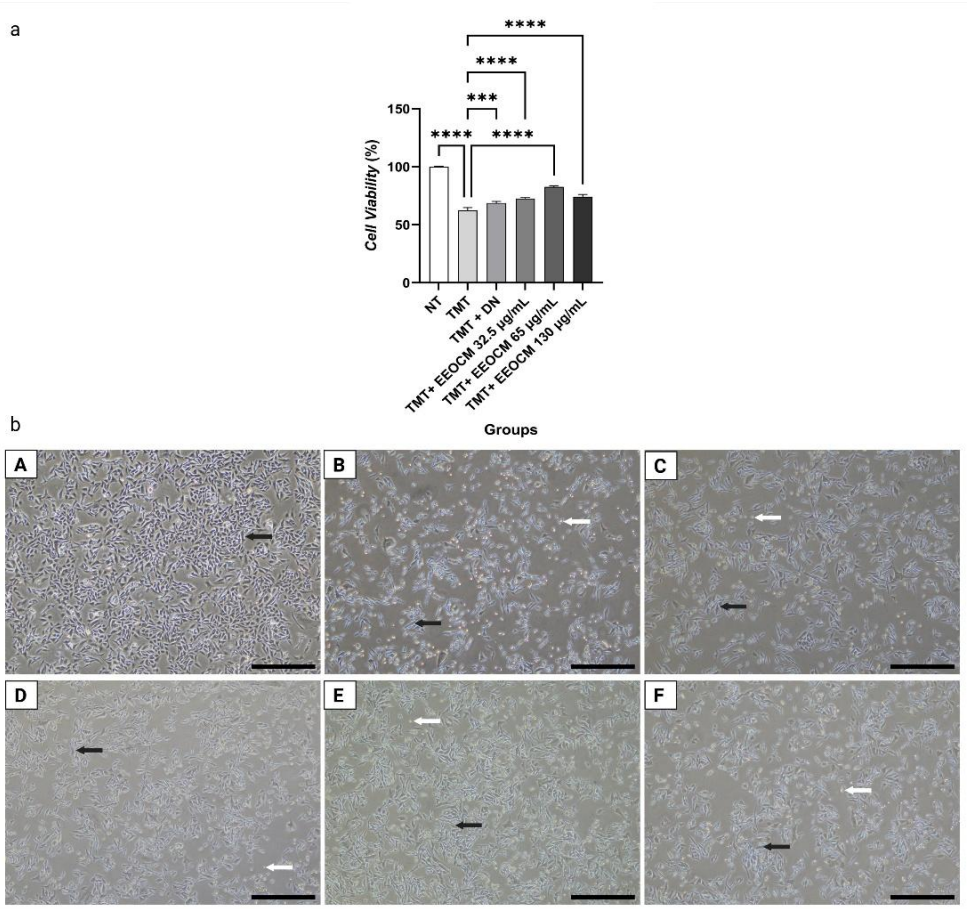


Figure 1 Polyherbal EEOCM extract increase the viability of the invitro model AD the PC12 cells in the presence of TMT. (a) Cell viability assay was measured by MTT testing, data are presented as mean ± SD from three independent experiments. Statistical significance was analyzed by one-way ANOVA followed by Tukey's post hoc test ($p < 0.05$, *$p < 0.01$, **$p < 0.001$, ***$p < 0.0001$, compared with the TMT-treated group). Among the treated groups, the 65 µg/mL polyherbal dose yielded the highest cell viability; (b) Morphology of TMT-Induced PC-12 Cells Across Treatment Groups. Representative microscopic images of PC-12 cells show that TMT exposure induced marked morphological degeneration, characterized by reduced cell density and the presence of non-viable cells. Among the treated groups, cells exposed to EEOCM at 65 µg/mL exhibited the most preserved morphology, closely resembling the untreated control group. Black arrow: Viable cell, white arrow: Non-viable cell. (A) Untreated, (B) TMT 10µM, (C) Donepezil 1 µM, (D) Polyherbal EEOCM 32.5 µg/mL, (E) Polyherbal EEOCM 65 µg/mL, (F) Polyherbal EEOCM 130 µg/mL. Scale bar: 500 µm.

The MTT assay demonstrated that treatment with the polyherbal extract improved the viability of TMT-exposed PC-12 cells in a concentration-dependent manner. To further support these findings, morphological assessment was conducted to provide qualitative confirmation of cellular integrity. Microscopic examination revealed that TMT induced clear degenerative changes in PC12 cells, whereas polyherbal treatment preserved structural features, consistent with the viability results (**Figure 1(b)**).

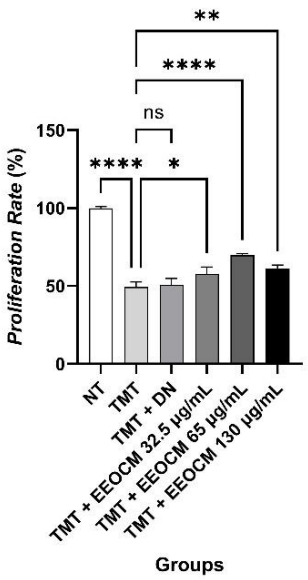


Figure 2 Polyherbal EEOCM Treatment Enhances Proliferation Rate in TMT-Exposed PC12 Cells. Data are presented as mean ± SD from three independent experiments. Statistical significance was analyzed by one-way ANOVA followed by Tukey's post hoc test (ns: Not significant, $p < 0.05$, *$p < 0.01$, **$p < 0.001$, ***$p < 0.0001$, compared with the TMT-treated group). The CCK-8 assay showed that polyherbal extract improved proliferation in a concentration-dependent manner, with EEOCM 65 µg/mL producing the highest proliferative effect.

Morphology assessment confirmed that polyherbal treatment preserved cellular structure under TMT-induced stress. To further evaluate whether these protective effects translated into enhanced cell growth, proliferation was quantified using the CCK-8 assay. The TMT exposure markedly reduced the proliferation rate of PC12 cells, whereas treatment with the polyherbal extract restored proliferation in a concentration-dependent manner (**Figure 2**). The CCK-8 assay demonstrated that polyherbal treatment restored the proliferation capacity of TMT-induced PC12 cells, with the intermediate dose showing the most pronounced effect.

Polyherbal EEOCM reduced nuclear damage and improved mitochondrial integrity on the TMT induced Alzheimer's disease on the PC-12 cell line

To further confirm whether increasing viability and proliferative of the invitro model AD were associated with protection against apoptosis, nuclear integrity was examined using Hoechst 33342 staining. Hoechst staining revealed fragmentation of the cells nucleus on the treated group (TMT induction-**Figure 3(a-B)** in compare to the treated group with EEOCM (**Figures 3(a-D)**, **3(a-E)**, and **3(a-F)**, the optimum dosage of EEOCM is 65 µg/mL (**Figure 3(a-E**) as same as of the cells condition in the presence of donepezil (**Figure 3(a-C)** and healthy cells (**Figure 3(a-A)**.

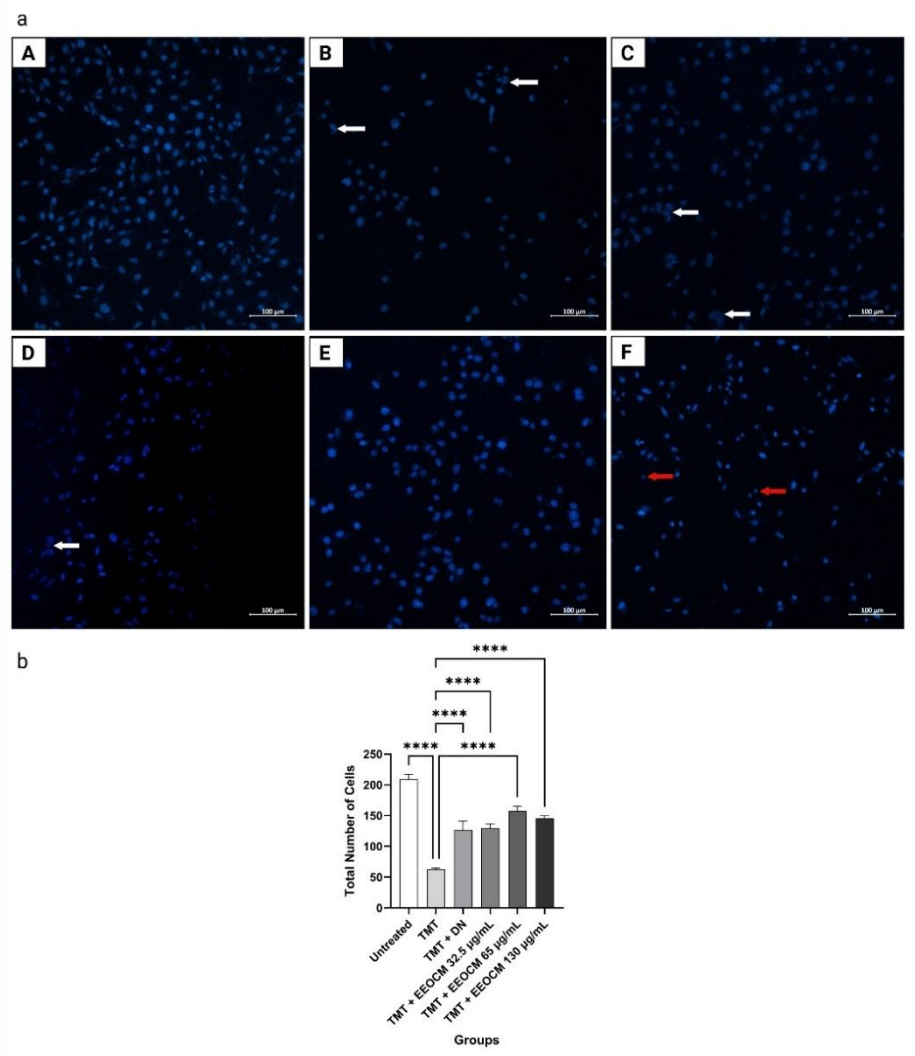


Figure 3 Polyherbal EEOCM Mitigates Apoptotic Nuclear Changes in TMT-Treated PC12 Cells (a) Morphologycal analysis by by Hoechst Assay described the untreated control group displayed the highest nuclear integrity, while TMT exposure show severe nuclear damage. Treatment with donepezil partially improved nuclear morphology as same as to polyherbal extract (EEOCM) at 32.5 µg/mL, The optimum dosage for the EEOCM is on the 65 µg/mL dose demonstrated the highest preservation of nuclear integrity among treated groups; (A) Untreated, (B) TMT 10µM, (C) Donepezil 1 µM, (D) Polyherbal EEOCM 32.5 µg/mL, (E) Polyherbal EEOCM 65 µg/mL, (F) Polyherbal EEOCM 130 µg/mL; White arrow: Fragmented nuclear, red arrow: Pyknosis nuclear; (b) Quantitative Cell Count of TMT-Induced PC12 Cells Following Polyherbal Treatment. Total cell numbers were quantified from Hoechst-stained images using ImageJ. Among the treated groups, EEOCM at 65 µg/mL preserved the highest cell count compared with other doses and donepezil. Data are expressed as mean ± SD (n = 5). ***$p < 0.001$, ****$p < 0.0001$, one-way ANOVA.

The alterations in nuclear morphology, prompting further assessment of mitochondrial function. JC-1 analysis demonstrated corresponding changes in mitochondrial membrane potential, indicating early cellular dysfunction associated with the treatment (**Figure 4**). The TMT induction reduced red fluorescence (**Figure 4(a-B)**, while polyherbal EEOCM treatment and Donepezil restored mitochondrial polarization, with the 65 µg/mL EEOCM dose showing the highest intensity among treatments (**Figures 4(a-C)** and **4(a-E)** In detailed the red fluorescence representing polarized mitochondria, green fluorescence indicates depolarized mitochondria where JC-1 exists in its monomeric form. Cells in the TMT-treated group exhibited smeared and weak green fluorescence, consistent with nuclear disintegration and reduced cell viability, whereas treatment with EEOCM and Donepezil reduced green fluorescence, reflecting

restoration of mitochondrial membrane potential, with the 65 µg/mL EEOCM dose showing the most pronounced effect (**Figure 4(b)**). Mitochondrial membrane potential was further quantified as the red/green JC-1 fluorescence ratio, an important indicator of mitochondrial health. TMT-induced cells showed a decreased ratio, indicating depolarization, whereas treatment with EEOCM and Donepezil increased the ratio, reflecting restoration of mitochondrial polarization (**Figure 4(d)**).

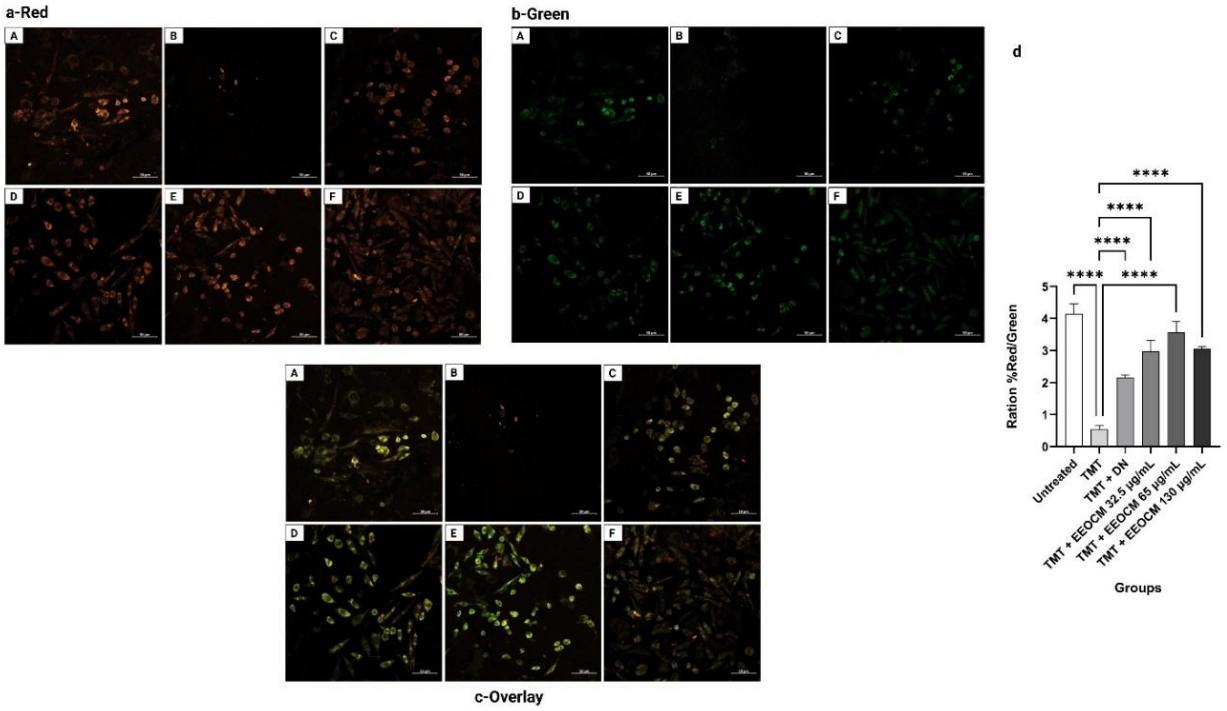


Figure 4 Mitochondrial Membrane Potential in Polyherbal EEOCM Treated PC-12 Cells on Confocal Microscopy Visualization (a) Mitochondrial Membrane Potential Indicated by JC-1 Red Fluorescence in Polyherbal-Treated PC12 Cells; (b) Mitochondrial Depolarization Indicated by JC-1 Green Fluorescence in Polyherbal Treated PC12 Cells; (c) The overlay visualization, TMT-induced cells exhibited decreased membrane potential, which was restored by polyherbal EEOCM treatment and Donepezil, the 65 µg/mL EEOCM dose demonstrating the highest mitochondrial polarization among the treatments; (A) Untreated, (B) TMT 10µM, (C) Donepezil 1 µM, (D) Polyherbal EEOCM 32.5 µg/mL, (E) Polyherbal EEOCM 65 µg/mL, (F) Polyherbal EEOCM 130 µg/mL; (d) Quantification of JC-1 Red/Green Ratio in PC12 Cells Following Polyherbal Treatment. The TMT-induced cells showed a decreased ratio, indicating mitochondrial depolarization, while EEOCM and Donepezil treatments restored the ratio, with 65 µg/mL EEOCM showing the highest recovery. Data are presented as mean ± SD; statistical significance was determined by one-way ANOVA followed by Tukey's post hoc test ($p < 0.05$, *$p < 0.01$, **$p < 0.001$, ***$p < 0.0001$, compared with the TMT-treated group).

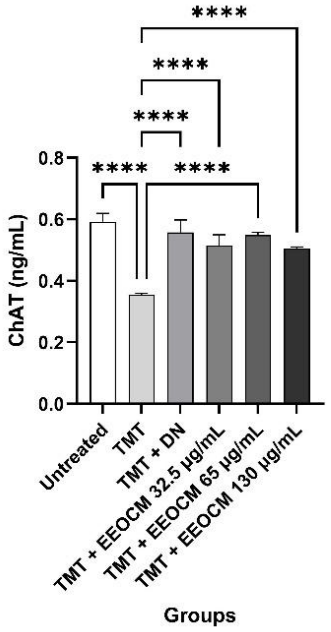
Morphological analysis by Hoechst staining exhibited a substantial decrease in nuclear condensation and fragmentation in treated Alzheimer's Disease Model-Rat Pheochromocytoma cell line (PC-12 cell line) compared to untreated controls, indicating that the extract combination effectively attenuated apoptosis. In parallel, JC-1 mitochondrial membrane potential analysis demonstrated that extract-treated cells maintained higher mitochondrial integrity, as evidenced by increased red fluorescence (aggregated JC-1) relative to green fluorescence (monomeric JC-1). Loss of mitochondrial membrane potential is a hallmark of the intrinsic apoptotic pathway, typically leading to cytochrome c release and caspase activation. The prevention of mitochondrial depolarization in this study suggests that the extract combination stabilizes mitochondrial function, there by inhibiting downstream apoptotic signalling [27,28].

Due to the results, the intriguing question is how the EEOCM may prevent apoptosis and promote

increasing of cell proliferation and viability, previous study has been shown that *Ocimum sanctum* possesses potent antioxidant, anti-inflammatory activities, which help to mitigate oxidative stress and neuroinflammation commonly associated with AD progression. Furthermore, *Ocimum sanctum* also promote upregulation of several neurotransmitter including serotonin, cholinacetyltransferase and neuropeptide Y [13-15,29,30]. Similarly, *Clitoria ternatea* has been shown to possess neuroprotective effects, primarily due to its flavonoid and anthocyanin content. These compounds exhibit acetylcholinesterase inhibitory activity, which can increase acetylcholine levels in the brain, a neurotransmitter often deficient in Alzheimer's patients. Elevated acetylcholine levels can aid in improving memory and learning [31]. Furthermore, extracts from *Clitoria ternatea* have been linked to upregulating neurotrophic factors that promote synaptic plasticity, thereby supporting cognitive functions and potentially reversing memory impairment associated with AD [31]. *Moringa oleifera* is particularly rich in polyphenols and flavonoids, known for their antioxidant properties. Studies have demonstrated that Moringa extracts can activate endogenous antioxidant defenses and significantly attenuate amyloid-β–induced neurotoxicity, which is a critical factor in Alzheimer's disease pathology [32]. The present findings are in agreement with these earlier observations where EEOCM polyherbals have a high content of flavonoids and polyphenols, but importantly, that extracts combining give a stronger protective effect in compared to each extract alone, this finding in concordance with the value on the formulation calculation of polyherbal which show the synergetic effect and no antagonist interaction.

Polyherbal EEOCM promote upregulation expression of BDNF and ChAT in TMT-induced Alzheimer's disease on the PC-12 cell line

The effects of EEOCM on neuronal biomarkers were evaluated by quantifying ChAT and BDNF levels in TMT-induced PC-12 cells using ELISA. TMT induction significantly reduced both ChAT and BDNF levels compared to untreated cells, indicating impaired cholinergic function and neurotrophic support. Treatment with EEOCM and Donepezil restored the levels of both biomarkers, with the 65 µg/mL EEOCM dose showing the most pronounced enhancement, comparable to Donepezil, suggesting optimal support of neuronal function and survival (**Figures 5** and **6**).



8

Figure 5 Polyherbal EEOCM Enhances ChAT Levels in TMT-Induced PC12 Cells. The TMT-induced cells showed a significant reduction in ChAT expression, whereas treatment with EEOCM and Donepezil restored ChAT levels. Data are presented as mean ± SD; statistical significance was determined by one-way ANOVA followed by Tukey's post hoc test ($p < 0.05$, *$p < 0.01$, **$p < 0.001$, ***$p < 0.0001$, compared with the TMT-treated group).

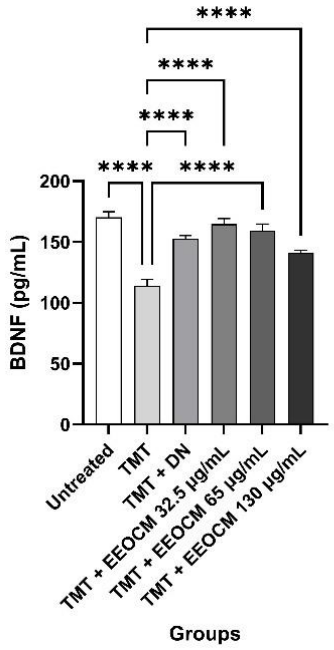


Figure 6 Polyherbal EEOCM Restores BDNF Expression in TMT-Induced PC12 Cells. Quantification of BDNF levels in PC12 cells by ELISA. TMT induction significantly decreased BDNF expression, while treatment with EEOCM and Donepezil restored BDNF levels. Data are presented as mean ± SD; statistical significance was determined by one-way ANOVA followed by Tukey's post hoc test ($p < 0.05$, *$p < 0.01$, **$p < 0.001$, ***$p < 0.0001$, compared with the TMT-treated group).

In addition, the results of morphological preservation (hoechts staining) and membrane potential analysis JC-1 is in line with the observed upregulation of the neuronal neurotrophic factor (BDNF) and neurotransmitter (ChAT), which play crucial roles in promoting neuronal survival and synaptic function. The upregulation of BDNF enhances neuronal resilience by activating TrkB-mediated signaling pathways, including the PI3K/Akt and MAPK/ERK pathways. Activation of these pathways supports cellular persistence and mitigating pro-apoptotic signaling, thus preventing neuronal loss [33,34]. Furthermore, BDNF has been shown to help maintain mitochondrial function and integrity, which is crucial for cell survival. Healthy mitochondria are essential for ATP production and regulation of apoptosis pathways. By preserving mitochondrial membrane potential, BDNF helps prevent the release of cytochrome c, which activates caspases involved in the apoptotic cascade. As an additional role BDNF has been identified to enhance glutamate synaptic vesicle exocytosis, thus promoting excitatory signaling, thus can enhance and maintain synaptic transmission, integrity and plasticity. This mechanism is important to support long-term potentiation (LTP) which is crucial for learning and memory [35,36].

At the same time, increased ChAT expression indicates improved cholinergic neurotransmission, which not only supports cognitive processes but also exerts neuroprotective effects by maintaining synaptic activity and reducing neuronal apoptotic to degeneration. The upregulation of ChAT observed in this study indicates an improvement in cholinergic neurotransmission, which is one of the most severely affected pathways in AD. Restoration of ChAT levels may enhance acetylcholine synthesis, thereby improving synaptic signaling and cognitive performance [37,38].

The results obtained in this study imply that a polyherbal approach may provide advantages more than single-compound interventions, as it offers multitarget protection against oxidative stress, neuroinflammation, cholinergic dysfunction, and neuronal apoptosis. The observed of synergistic effect of the extracts underline the importance of exploring combination therapies

derived from medicinal plants as complementary strategies to conventional treatments. Nevertheless, while the *in vitro* findings are promising, further studies are required to validate these effects *in vivo* and to elucidate the pharmacokinetics, bioavailability, and safety of the extract combination. Future work should also investigate the molecular signalling pathways linking extract treatment to ChAT and BDNF upregulation, including the possible involvement of CREB, PI3K/Akt, and MAPK/ERK pathways. Such insights will be essential for advancing the translational potential of these polyherbal extracts in the development of novel, plant-based therapeutic options for AD.

Donepezil was included in this study as a reference compound to contextualize the observed neuroprotective and cholinergic-related effects of the polyherbal formulation. Through multiple assays, including cell viability, mitochondrial function, nuclear morphology, and the expression of BDNF and ChAT, donepezil provided a useful benchmark under *in vitro* AD-related neurotoxicity conditions. However, it should be noted that the aim was not to establish direct equivalence in efficacy or to fully elucidate mechanistic similarities between donepezil and the polyherbal formulation, but rather to support the interpretation of the observed biological effects.

Conclusions

Taken together, the results suggest a mechanistic model in which the combined extracts (Ocimum sanctum, Clitoria ternatea, and Moringa oleifera) prevent neuronal apoptosis in PC12 cells through suppression of nuclear fragmentation and chromatin condensation, stabilization of mitochondrial membrane potential, and upregulation of neurotrophic and cholinergic markers (BDNF and ChAT). These converging actions highlight the multitarget potential of the extract combination to counteract oxidative stress and apoptotic pathways, ultimately enhancing neuronal survival in an Alzheimer's disease cellular model (Rat Pheochromocytoma cell line).

Acknowledgements

The Integrated Laboratory of Research and Testing (LPPT Universitas Gadjah Mada, Yogyakarta 55281, Indonesia) is acknowledged by the writers. The Ministry of Education, Culture, Research, and Technology provided funding for this work through Regular Fundamental Research under Grant number 2423/UN1/DITLIT/Dit-Lit/PT.01.03/2025.

Declaration of Generative AI in Scientific Writing

In preparing this manuscript, the authors utilized ChatGPT (OpenAI) and SciSpace as editorial support. Their use was limited to refining the English language, correcting grammatical and stylistic issues, and assisting with the selection and verification of citations. No AI tool was used to generate scientific findings, conduct data analysis, or interpret the results. All scientific content was developed and reviewed by the authors, who take full responsibility for the integrity and conclusions of the manuscript.

CRediT author statement

Wilda Bunga Tina Sanjaya: Investigation; Visualization; Methodology; Software. **Hevi Wihadmadyatami**: Supervision; Data Curation; Validation; Writing - Review & Editing. **Dwi Aris Agung Nugrahaningsih**: Formal analysis; Project administration. **Rini Widayanti**: Supervision; Data Curation. **Ulayatul Kustiati**: Software; Validation. **Dinda Aliffia**: Visualization; Methodology. **Sadad Faisal Faiz**: Formal analysis. **Dwi Liliek Kusindarta**: Conceptualization; Supervision; Validation; Resources.

References

[1] T Earnest, B Yang, D Kothapalli and A Sotiras. Comprehensive evaluation of AT(N) imaging biomarkers for predicting cognition. *medRxiv* 2024. https://doi.org/10.1101/2024.11.25.24317943

[2] CRJ Jr, DA Bennett, K Blennow, MC Carrillo, B Dunn, SB Haeberlein, DM Holtzman, W Jagust, F Jessen, J Karlawish, E Liu, JL Molinuevo, T Montine, C Phelps, KP Rankin, CC Rowe, P Scheltens, E Siemers, HM Snyder, R Sperling, ..., N Silverberg. NIA-AA Research Framework: Toward a biological definition of Alzheimer's disease. *Alzheimer's & Dementia* 2018; **14(4)**, 535-562.

[3] SC Burnham, PM Coloma, QX Li, S Collins, G Savage, S Laws, J Doecke, P Maruff, RN Martins, D Ames, CC Rowe, CL Masters and VL Villemagne. Application of the NIA-AA research

framework: Towards a biological definition of Alzheimer's disease using cerebrospinal fluid biomarkers in the AIBL study. *The Journal of Prevention of Alzheimer's Disease* 2019; **6(4)**, 248-255.

[4] SJ Yim, S Yasar, N Schoenborn and E Lang. Expanded disease definitions in Alzheimer's disease and the new era of disease-modifying drugs. *BMJ Evidence-Based Medicine* 2025; **30(5)**, 288-290.

[5] S Toniolo, FD Lorenzo, S Bernardini, NB Mercuri and GM Sancesario. Blood–Brain barrier dysfunction and Aβ42/40 ratio dose-dependent modulation with the ApoE Genotype within the ATN Framework. *International Journal of Molecular Sciences* 2023; **24(15)**, 12151.

[6] M Franczak. Alzheimer disease: What's new, what's true? Available at: https://tressless.com/research/alzheimers-disease-new-insights-truths-7RzG, accessed January 2024.

[7] R Wang. Global Burden of Alzheimer's disease and other dementias during 1990 - 2021: A Global Burden of disease and risk factors study 2021-based study. *Neuroepidemiology* 2025; **60(1)**, 16-27.

[8] Y Turana, J Tengkawan, I Suswanti, DY Suharya, W Riyadina and J Pradono. Primary prevention of Alzheimer's disease in Indonesia. *International Journal of Aging Research* 2019; **2**, 40.

[9] J Tanoey and H Becher. Diabetes prevalence and risk factors of early-onset adult diabetes: Results from the Indonesian family life survey. *Global Health Action* 2021; **14(1)**, 2001144.

[10] MPG Moreta, N Burgos-Alonso, M Torrecilla, J Marco-Contelles and C Bruzos-Cidón. Efficacy of acetylcholinesterase inhibitors on cognitive function in Alzheimer's disease. Review of Reviews. *Biomedicines* 2021; **9(11)**, 1689.

[11] C Fruchtengarten, LMVRE Ribeiro, MM Schichman, BPBD Souza, DMAD Sousa, GDM Vieira, DFD Arruda, LFEVDM Fernandes, JPS Barbara, LM Gaissler, RL Silva and CSDM Pereira. Pharmacological treatment of Alzheimer's disease: An integrative review on the effectiveness of cholinesterase and memantine inhibitors. *International Journal of Health Science* 2023; **3(41)**, 15934123010610.

[12] V Marinho, E Bertrand, R Naylor, I Bomilcar, J Laks, A Spector and DC Mograbi. Cognitive stimulation therapy for people with dementia in Brazil (CST-Brasil): Results from a single blind randomized controlled trial. *The International Journal of Geriatric Psychiatry* 2021; **36(2)**, 286-293.

[13] U Kustiati, TSD Ratih, NDA Agung, DL Kusindarta and H Wihadmadyatami. *In silico* molecular docking and *in vitro* analysis of ethanolic extract *Ocimum sanctum* Linn.: Inhibitory and apoptotic effects against non-small cell lung cancer. *Veterinary World* 2021; **14(12)**, 3175-3178.

[14] D Aliffia, DA Ramadhani, W Wasityastuti, DRT Sari, U Kustiati, H Wihadmadyatami, and DL Kusindarta. *Ocimum sanctum* leaves prevent neuronal cell apoptosis through reduction of Caspase-3 and -9 expressions and inhibition of β-amyloid oligomerization. *Indonesian Biomedical Journal* 2023; **15(4)**, 322-332.

[15] MBA Mataram, P Hening, FN Harjanti, S Karnati, W Wasityastuti, DAA Nugrahaningsih, DL Kusindarta and H Wihadmadyatami. The neuroprotective effect of ethanolic extract *Ocimum sanctum* Linn. in the regulation of neuronal density in hippocampus areas as a central autobiography memory on the rat model of Alzheimer's disease. *Journal of Chemical Neuroanatomy* 2021; **111**, 101885.

[16] A Villarruel-López, DALL Mora, OD Vazquez-Paulino, AG Puebla-Mora, MR Torres-Vitela, LA Guerrero-Quiroz and K Nuno. Effect of *Moringa oleifera* consumption on diabetic rats. *BMC Complementary and Alternative Medicine* 2018; **18**, 127.

[17] BD Tambe and PD Gadhave. Phytochemical screening and *in vitro* antibacterial activity of *Moringa oleifera* (Lam.) leaf extract. *International Journal of Science and Research Archive* 2024; **12(1)**, 125-130.

[18] WBT Sanjaya, DR Tirtosari, R Widayanti, DAA Nugrahaningsih, GR Saragih, H Wihadmadyatami and DL Kusindarta. Characterization of phytochemicals of *Clitorea ternatea* and the

potention as neuroprotectant to prevent Alzheimer's disease. *Biodiversitas* 2025; **26(7)**, 3144-3159.

[19] MY Ali, MI Khalil, FN Jahan, MB Hossain and AK Samanta. *Moringa oleifera*: A review on nutritional attributes, therapeutic applications and value-added product generation. *SAARC Journal of Agriculture* 2022; **20(2)**, 63447.

[20] S Dubey and AK Dixit. Preclinical evidence of polyherbal formulations on wound healing: A systematic review on research trends and perspectives. *Journal of Ayurveda and Integrative Medicine* 2023; **14(2)**, 100688.

[21] VL Yap, LF Tan, M Rajagopal, C Wiart, M Selvaraja, MY Leong and PL Tan. Evaluation of phytochemicals and antioxidant potential of a new polyherbal formulation TC-16: Additive, synergistic or antagonistic? *BMC Complementary Medicine and Therapies* 2023; **23**, 39.

[22] MC Rîmbu, L Popescu, M Mihaila, RC Sandulovici, D Cord, CM Mihailescu, ML Galatanu, M Panturoiu, CE Manea, A Boldeiu, O Brincoveanu, M Savin, A Grigoroiu, FD Ungureanu, E Amzoiu, M Popescu and E Truta. Synergistic effects of green nanoparticles on antitumor drug efficacy in hepatocellular cancer. *Biomedicines* 2025; **13(3)**, 641.

[23] LC Crowley, BJ Marfell, and NJ Waterhouse. Analyzing cell death by nuclear staining with Hoechst 33342. *Cold Spring Harbor Protocols* 2016; **2016(9)**, 778-782.

[24] D Velásquez-Jiménez, DA Corella-Salazar, BS Zuñiga-Martínez, JA Domínguez-Avila, M Montiel-Herrera, NJ Salazar-López, J Rodrigo-Garcia, MA Villegas-Ochoa and GA González-Aguilar. Phenolic compounds that cross the blood–brain barrier exert positive health effects as central nervous system antioxidants. *Food & Function* 2021; **12(21)**, 10356-10369.

[25] R Shimazu, M Anada, A Miyaguchi, Y Nomi and H Matsumoto. Evaluation of blood-brain barrier permeability of polyphenols, anthocyanins, and their metabolites. *Journal of Agricultural and Food Chemistry* 2021; **69(39)**, 11676-11686.

[26] JD Sánchez-Martínez, A Valdés, R Gallego, ZJ Suárez-Montenegro, M Alarcón, E Ibañez, G Alvarez-Rivera and A Cifuentes. Blood-brain barrier permeability study of potential neuroprotective compounds recovered from plants and Agri-food by-Products. *Frontier in Nutrition* 2022; **9**, 924596.

[27] YJ Wu, BS Wong, SH Yea, CI Lu and SH Weng. Sinularin induces apoptosis through mitochondria dysfunction and inactivation of the pI3K/Akt/mTOR pathway in Gastric carcinoma cells. *Marine Drugs* 2016; **14(8)**, 142.

[28] EM El-Sheref, AA Aly, MB Alshammari, AB Brown, SMN Abdel-Hafez, WY Abdelzaher, S Brase and EMN Abdelhafez. Design, synthesis, molecular docking, antiapoptotic and Caspase-3 Inhibition of New 1,2,3-Triazole/*Bis*-2(1*H*)-Quinolinone Hybrids. *Molecules* 2020; **25(21)**, 5057.

[29] MN Raditya, AMM Bagus, U Kustiati, H Wihadmadyatami and DL Kusindarta. Data of the expression of serotonin in Alzheimer's disease (AD) rat model under treatment of ethanolic extract *Ocimum sanctum* Linn. *Data in Brief* 2020; **30**, 105654.

[30] DL Kusindarta, H Wihadmadyatami and A Haryanto. The analysis of hippocampus neuronal density (CA1 and CA3) after *Ocimum sanctum* ethanolic extract treatment on the young adulthood and middle age rat model. *Veterinary World* 2018; **11(2)**, 135-140.

[31] KN Jiji and P Muralidharan. Neuroprotective effects of *Clitoria ternatea* L. against propionic acid-induced behavior and memory impairment in autistic rat model. *Future Journal of Pharmaceutical Sciences* 2021; **7**, 163.

[32] M Mundkar, A Bijalwan, D Soni and P Kumar. Neuroprotective potential of *Moringa oleifera* mediated by NF-kB/Nrf2/HO-1 signaling pathway: A review. *Journal of Food Biochemistry* 2022; **46(12)**, e14451.

[33] J Matsubayashi, Y Kawaguchi, Y Kawakami and K Takei. Brain-derived neurotrophic factor (BDNF) induces antagonistic action to Nogo signaling by the upregulation of lateral olfactory tract usher substance (Lotus) expression. *Journal of Neurochemistry* 2023; **164(1)**, 29-43.

[34] A Hidayat, M Arief, A Wijaya and S As'ad. Vascular endothelial growth factor and brain-derived neurotropic factor levels in ischemic

stroke subject. *Indonesian Biomedical Journal* 2016; **8(2)**, 115-118.

[35] RA Williams, KW Johnson, FS Lee, HCH Jr and J Platholi. A common human brain-derived neurotrophic factor polymorphism leads to sustained depression of excitatory synaptic transmission by isoflurane in hippocampus. *bioRxiv* 2022. https://doi.org/10.1101/2021.12.30.474566

[36] SMG Solinas, E Edelmann, V Leßmann and M Migliore. A kinetic model for brain-derived neurotrophic factor mediated spike timing-dependent LTP. *PLoS Computational Biology* 2019; **15(4)**, e1006975.

[37] H Fgaier, IHI Mustafa, AAR Awad and A Elkamel. Modeling the interaction between β-Amyloid aggregates and choline acetyltransferase activity and its relation with cholinergic dysfunction through two-enzyme/two compartment model. *Computational and Mathematical Methods in Medicine* 2015; **2015**, 923762.

[38] MR Gielow and L Zaborszky. The input-output relationship of the cholinergic basal forebrain. *Cell Reports* 2017; **18(7)**, 1817-1830.